Inorg. Chem. **2005**, *44*, 1421−1424

Selective Generation of Organic Aggregates Included within Metal−Organic Micropores through Vapor Adsorption

Satoshi Takamizawa,* Teruo Saito, Takamasa Akatsuka, and Ei-ichi Nakata

Yokohama City University, Graduate School of Integrated Science, Kanazawa-ku, Yokohama 236-0027, Japan

Received November 22, 2004

The ethanol vapor adsorption behavior and the inclusion crystal structure of a 1D-transformable coordination polymer host were characterized. The adsorption jump was observed during phase transition or two-phase equilibrium with abnormal adsorption enthalpy caused by the nature of "mass induced phase transition." The included ethanol guests selectively form O–H···O hydrogen bonded pairs inside channels, suggesting selective construction of a specific cluster/aggregate in pores under control of thermodynamic factors and cooperative intermolecular interactions among the guest and channel surface.

Introduction

The recent increase in research into metal−organic crystalline host solids is due to their specific properties such as guest exchange and gas adsorption.[1] The essential nature of the host transformation induced by guest inclusion is of great interest.[2−9] Recently, we found single-crystal adsorbents of metal(II) benzoate pyrazine, $[M^{II}_2(bza)_4(pyz)]_n$ (bza and pyz = benzoate and pyrazine, M = Cu (**1**)[10] and Rh[11]), which are suitable for the study of guest-containing crystal structures through gas adsorption.[12,13] To elucidate the control ability for constructing a guest cluster/aggregate of single-crystal adsorbents, we attempted to prepare an ethanol inclusion crystal through gas adsorption due to its certain vapor pressure and unsymmetrical structure with amphipathicity, which would construct a specific aggregate in hydrophobic

* To whom correspondence should be addressed. Tel & fax: 81-45-787-2187. E-mail: staka@yokohama-cu.ac.jp.

(1) (a) Fujiwara, M.; Seki, K.; Mori, W.; Takamizawa, S. Patent Nos. JP 09132580, 1995; EP 0727608, 1996. (b) Mori, W.; Inoue, F.; Yoshida, K.; Nakayama, H.; Takamizawa, S.; Kishita, M. *Chem. Lett.* **1997**, *1997*, 1219−1220. (c) Kondo, M.; Yoshitomi, T.; Seki, K.; Matsuzaka, H.; Kitagawa, S. *Angew. Chem., Int. Ed. Engl.* **1997**, *36*, 1725. (d) Li, H.; Eddaoudi, M.; Groy, T. L.; Yaghi, O. M. *J. Am. Chem. Soc.* **1998**, *120*, 8571−8572. (e) Yaghi, O. M.; O'Keeffe, M.; Ockwig, N. W.; Chae, H. K; Eddaoudi, M.; Kim, J. *Nature* **2003**, *423*, 705−714. (f) Manakov, A. Y.; Soldatov, D. V.; Ripmeester, J. A.; Lipkowski, J. *J. Phys. Chem. B* **2000**, *104*, 12111−12118. (g) Li, D.; Kaneko, K. *J. Phys. Chem. B* **2000**, *104*, 8940−8945. (h) Mori, W.; Takamizawa, S. In *Organometallic Conjugation*; Nakamura, A., Ueyama, N., Yamaguchi, K., Eds.; Kodansha Springer: Tokyo, 2002; Chapter 6, pp 179−213.

(2) (a) Soldatov, D. V.; Ripmeester, J. A.; Shergina, S. I.; Sokolov, I. E.; Zanina, A. S.; Gromilov, S. A.; Dyadin, Y. A. *J. Am. Chem. Soc.* **1999**, *121*, 4179−4188. (b) Soldatov, D. V.; Grachev, E. V.; Ripmeester, J. A. *Cryst. Growth Des.* **2002**, *2*, 401−408.

(3) Makinen, S. K.; Melcer, N. J.; Parvez, M.; Shimizu, G. K. H. *Chem.−Eur. J.* **2001**, *7*, 5176−5182.

(4) (a) Fletcher, A. J.; Cussen, E. J.; Bradshaw, D.; Rosseinsky, M. J.; Thomas, K. M. *J. Am. Chem. Soc.* **2004**, *126*, 9750−9759. (b) Cussen, E. J.; Claridge, J. B.; Rosseinsky, M. J.; Kepert, C. J. *J. Am. Chem. Soc.* **2002**, *124*, 9574−9581. (c) Kepert, C. J.; Rosseinsky, M. J. *Chem. Commun.* **1999**, 375−376. (d) Kepert, C. J.; Hesek, D.; Beer, P. D.; Rosseinsky, M. J. *Angew. Chem., Int. Ed.* **1998**, *37*, 3158−3160. (e) Fletcher, A. J.; Cussen, E. J.; Prior, T. J.; Rosseinsky, M. J.; Kepert, C. J.; Thomas, K. M. *J. Am. Chem. Soc.* **2001**, *123*, 10001−10011.

(5) Beauvais, L. G.; Shores, M. P.; Long, J. R. *J. Am. Chem. Soc.* **2000**, *122*, 2763−2772.

(6) Suh, M. P.; Ko, J. W.; Choi, H. J. *J. Am. Chem. Soc.* **2002**, *124*, 10976−10977.

(7) Abrahams, B. F.; Jackson, P. A.; Robson, R. *Angew. Chem., Int. Ed.* **1998**, *37*, 2656−2659.

(8) (a) Matsuda, R.; Kitaura, R.; Kitagawa, S.; Kubota, Y.; Kobayashi, T. C.; Horike, S.; Takata, M. *J. Am. Chem. Soc.* **2004**, *126*, 14063−14070. (b) Kitaura, R.; Seki, K.; Akiyama, G.; Kitagawa, S. *Angew. Chem., Int. Ed.* **2003**, 428−431.

(9) (a) Biradha, K.; Fujita, M. *Angew. Chem., Int. Ed.* **2002**, *41*, 3392−3395. (b) Biradha, K.; Hongo, Y.; Fujita, M. *Angew. Chem., Int. Ed.* **2002**, *41*, 3395−3398.

(10) Takamizawa, S.; Nakata, E.; Yokoyama, H. *Inorg. Chem. Commun.* **2003**, *6*, 763−765.

(11) Takamizawa, S.; Hiroki, T.; Nakata, E.; Mochizuki, K.; Mori, W. *Chem. Lett.* **2002**, *2002*, 1208−1209.

(12) (a) Takamizawa, S.; Nakata, E.; Yokoyama, H.; Mochizuki, W.; Mori, *Angew. Chem., Int. Ed.* **2003**, *36*, 4331−4334. (b) Takamizawa, S.; Nakata, E.; Saito, T. *Inorg. Chem. Commun.* **2004**, *7*, 1−3. (c) Takamizawa, S.; Nakata, E.; Saito, T. *Angew. Chem., Int. Ed.* **2004**, *43*, 1368−1371. (d) Takamizawa, S.; Nakata, E.; Saito, T.; Akatsuka, T.; Kojima, K. *CrystEngComm* **2004**, *6*, 197−199. (e) Takamizawa, S.; Nakata, E.; Saito, T.; Kojima, K. *CrystEngComm* **2003**, *5*, 411−413. (f) Takamizawa, S.; Nakata, E.; Saito, T. *Inorg. Chem. Commun.* **2003**, *6*, 1415−1418.

(13) (a) Takamizawa, S.; Nakata, E.; Saito, T. *CrystEngComm* **2004**, *6*, 39−41. (b) Takamizawa, S.; Nakata, E.; Saito, T. *Chem. Lett.* **2004**, *33*, 538−539.

10.1021/ic048351s CCC: $30.25
Published on Web 01/27/2005

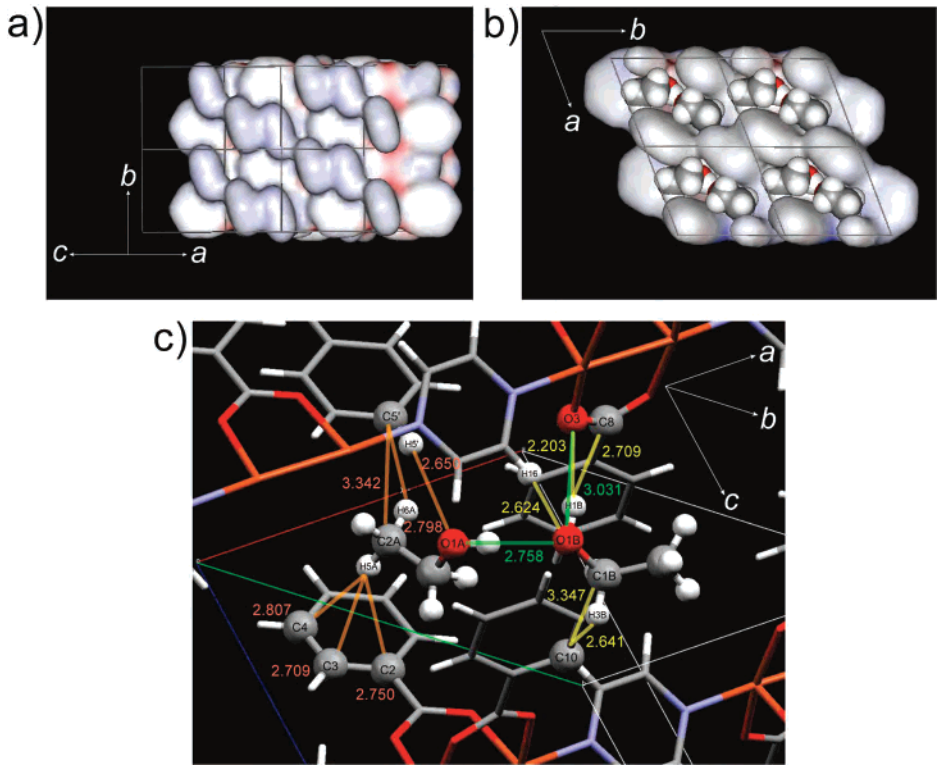

Figure 1. Surface view of empty **1** (left, *C*2/*c*) [ref 10] (a) and ethanol inclusion crystal structure **1**·2(C_2H_5OH) (right, $P\bar{1}$) (b) and environment of included ethanol with short contact interatomic distances (Å) (c).

channels by enhancing intermolecular hydrophilic interactions.

Experimental Section

Single-Crystal X-ray Diffraction Experiment. Single-crystal X-ray analysis was performed on a Bruker Smart APEX CCD area diffractometer with a nitrogen-flow temperature controller using graphite-monochromated Mo Kα radiation (λ = 0.71073 Å). The capillary was mounted and then cooled in a cold nitrogen stream after single crystal **1** was exposed to ethanol vapor at room temperature. Empirical absorption corrections were applied using the SADABS program. The structures were solved by direct methods (SHELXS 97) and refined by full-matrix least-squares calculations on F^2 (SHELXL-97) using the SHELX-TL program package. Non-hydrogen atoms were refined anisotropically; hydrogen atoms were fixed at calculated positions. The H-bonded ethanol aggregate presents centrosymmetric disorder (see Supporting Information) CCDC-235081.

Adsorption Measurement. The ethanol vapor adsorption isotherm curves were measured on a Quantachrome Autosorb-1-VP in a relative pressure (P/P_0, P_0 = saturation vapor pressure) range from 10^{-2} to 0.9 (using P_0 = 44.06, 32.42, 23.55, and 16.88 mmHg at 20, 15, 10, and 5 °C, respectively).

Results and Discussion

Crystal Structure under the EtOH Inclusion State. Crystals of $[Cu^{II}_2(bza)_4(pyz)]_n$ (**1**) were prepared by the method previously reported[10] (see Table 1). X-ray diffraction measurement for **1** with ethanol vapor reveals the formation of an ethanol inclusion crystal of **1**·2(C_2H_5OH), which was determined at 90 K with the $P\bar{1}$ space group, accompanying the crystal phase transition from α(monoclinic) to β(triclinic) lattice with various gaseous guests as previous reported.[12,13]

Table 1. Crystallographic Data for Single-Crystal Host **1** under the Condition of Vapor Adsorption

complex	**1**·2(C_2H_5OH)
color and shape	blue plate
dimension/mm^3	0.62 × 0.20 × 0.10
empirical formula	$C_{36}H_{36}Cu_2N_2O_{10}$
M/g mol^{-1}	783.77
crystal system	triclinic
space group (number)	$P\bar{1}$ (No. 2)
T/K	90
a/Å	9.6813(12)
b/Å	10.3897(13)
c/Å	10.7623(14)
α/deg	71.088(3)
β/deg	64.816(2)
γ/deg	63.731(2)
V/Å^3	866.08(19)
Z	1
D_{calcd}/Mg m^{-3}	1.503
μ(Mo Kα)/mm^{-1}	1.011
independent reflections (R_{int})	4201(0.0212)
R1 ($I > 2\sigma$ (all data))	0.0690(0.0735)
wR2 ($I > 2\sigma$ (all data))	0.1835(0.1855)
leastdiff. peak (hole)/e Å^{-3}	1.833 (−0.954)

The included ethanol molecules are coherently aligned in a linear fashion in regularly forming hydrogen bonded pairs along the expanded channels by the flexibility of the host lattice (Figure 1a,b), which is stabilized in cooperative interaction among guest and channel. The hydrophilic interaction stations OH moieties of ethanol on the carboxylate O(3) of the host lattice to form an O−H(guest)···O−H(guest)···O(host) hydrogen bond core with strong guest−guest aggregation (O···O, 2.758(13) Å) and weak host−guest hanging (3.031(10) Å), subsequently assisted by a hydrogen bond from the surrounding pyrazine and benzene rings of the channel surface. The hydrophobic alkyl moieties of the

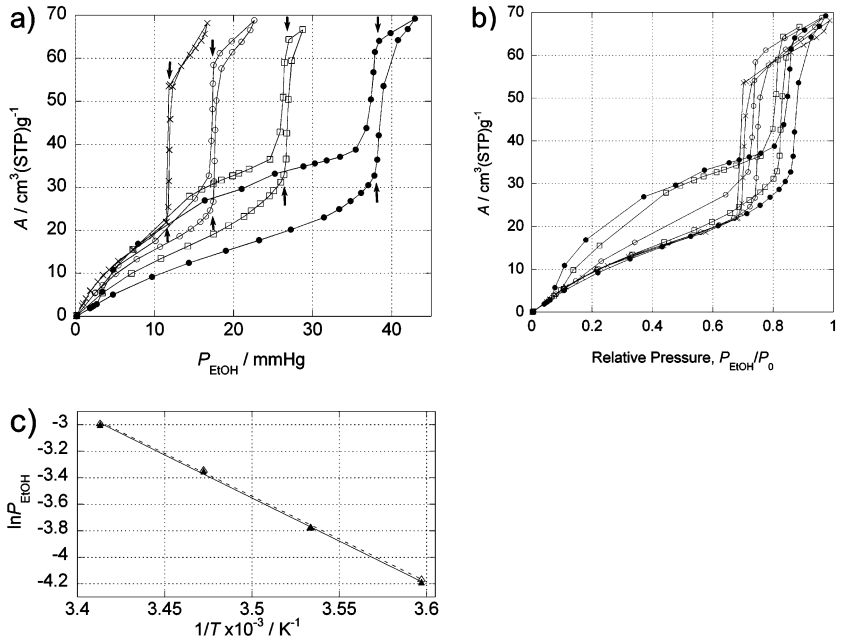

Figure 2. Ethanol vapor sorption curves for **1** at 5 (×), 10 (○), 15 (□), and 20 °C (●) with absolute pressure axis (a) and with relative pressure axis (b) (using P_0 (saturation vapor pressure) = 44.06, 32.42, 23.55, 16.88 mmHg at 20, 15, 10, and 5 °C, respectively) and linearity in the Clausius−Clapeyron correlation for the starting gas pressures of discontinuous sorption behavior (c). (*A*: amount of adsorbed ethanol. Vapor pressures for the calculation result in panel c are indicated by arrows inset on the starting points in panel a.)

guests positively contact the conjugated planes of the channel surface through alkyl(methyl/methylene)···π intermolecular interactions (Figure 1c). This is the precise structural determination for selective construction of regular aggregates in microporous compounds through the gas-adsorption process.

Surprisingly, the included ethanol guests only form the tail (−OH) to tail hydrogen bonded pairs. Considering the difficulty for the large ethanol molecules to turn around and substitution of the order within the narrow 1-D channels, the ethanol guest should insert in alternate molecular directions of head and tail at the channel entrance and most likely transfers in the channel to maintain the aggregated pair structure. Considering the smooth diffusion for the tightly confined long ethanol pair inside the narrow channel, the surface motion may play an important role in guest transfer, which was suggested in the results for other guests.[13]

Ethanol Vapor Adsorption Property. Vapor sorption isotherm measurement revealed a smooth and reversible adsorption ability of **1** for ethanol vapor at 5−20 °C (Figure 2a,b). A two-step adsorption property with a significant jump was observed in the adsorbed amount between ca. 20 and 60 cm^3 (STP) g^{-1}, caused by the change in the channel structure. The amount of adsorbed ethanol in **1** nearly reaches saturation vapor pressure at each temperature to a maximum of 69 cm^3 (STP) g^{-1} or 2.1 ethanol molecules per Cu_2 unit (32.3 cm^3 g^{-1} = ethanol/Cu_2), which agrees well with the chemical composition determined by X-ray diffraction analysis. Although the region of the adsorption jump shifted to a higher relative pressure region as the temperature increased, this shows that **1** finally reaches the same stable phase by ethanol adsorption at each temperature. The specific hysteresis below the region of the jump appears at a higher temperature, indicating a different method of guest transfer in the desorption process, which might be caused by transfer of the isolated ethanol due to cleavage of the hydrogen bond by thermal activation. The area of adsorption jump decreases as the temperature increases, indicating that a supercritical state exists beyond the critical point of the vanishing of the two-phase equilibrium state.

Description of Crystal Phase Transition. Although the rearrangement of the crystal structure seems to be complex, the adsorption isotherm curve provides the essential information for elucidating the nature of the phase transition of **1**. The natural logarithm of the vapor pressure ($\ln P_{EtOH}$) at the starting points of the adsorption and desorption jumps and the reciprocal measuring temperatures (T^{-1}) show a good linear correlation coincident with the Clausius−Clapeyron equation[14] (Figure 2c). This relationship clearly shows that the observed jump area has the same ΔH of 53.9 kJ mol^{-1} in a wide temperature range. This correlation gives the isosteric heat of adsorption (ΔH_{iso}) using two isotherm curves at different temperatures for the same adsorption quantity. Thus, the *A* (adsorption amount)−ΔH_{iso} curve for **1** was numerically estimated by the equation using two adsorption curves at 10 and 20 °C (Figure 3a). The enthalpy leaps were clearly observed around the initial and terminal regions of the adsorption jump, and a plateau exists between them. The discontinuous leap of enthalpy indicates the first-order phase transition of **1**. The plateau indicates the coexistence of the α- and β-crystal phases, where the propagation of the β-crystal phase continues as the adsorption amount increases to display the same situation for gas adsorption. Therefore, the differential of ΔH_{iso} shows two peaks, which can be used as an index for the initial and terminal points of the

(14) $d(\ln P)/d(T^{-1}) = \Delta H/R$ for the adsorption process, where *R* and ΔH denote the gas constant and adsorption enthalpy of the guest, respectively.

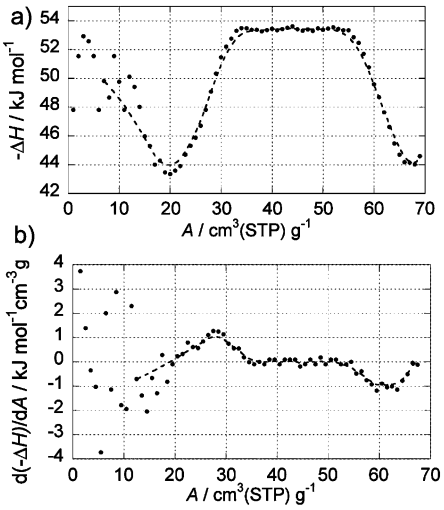

Figure 3. A vs $-\Delta H$ (a) and A vs $(-\Delta H)'$ curves (b) numerically calculated using the Clausius−Clapeyron equation for adsorption curves at 10 and 20 °C in Figure 2 (A: amount of adsorbed ethanol).

coexistence of the two crystal phases (Figure 3b). The ratio of $\alpha-\beta$ phases should be determined by the adsorption fraction in the range of A_{pro}, which can be controlled by the guest supply (see Figure 4). In the $\alpha-\beta$ phase equilibrium, the adsorption amount actually increases at the $\alpha-\beta$ phase boundary, which should have a fluctuating and changeable structure. The abnormal adsorption enthalpy during phase equilibrium may be correlated with the dynamic property of the phase boundary.

The current phase transition is essentially caused by the adsorption phenomenon. Thus, the observed phenomenon is clearly defined as "mass (amount of adsorbed guest) induced phase transition" in changing chemical composition triggered by gas clathrate formation (Figure 4). The transformation property through the adsorption process is most likely characterized by a combination of phase boundary transfer and guest diffusion methods, which provide specific adsorption behavior.

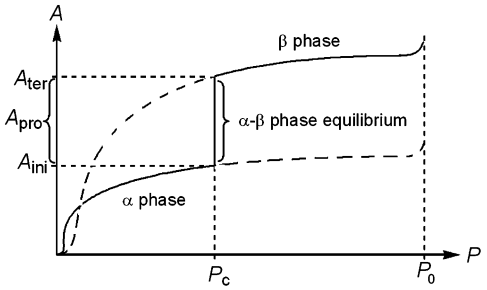

Figure 4. Adsorption curve for mass induced $\alpha-\beta$ phase transition with equilibrium scheme (P_c, critical pressure; P_0, saturation pressure; A_{ini}, initial adsorption amount of transition; A_{ter}, terminal adsorption amount of transition; A_{pro}, adsorption amount in phase equilibrium state).

Conclusion

The current transformation property of single-crystal adsorbent behavior is clearly defined as a "mass induced phase transition" through gas clathrate formation. The selective construction ability of various clusters/aggregates inside the pores is also elucidated. This procedure has the potential for producing various clusters/aggregates in the set of a single-crystal adsorbent and preferred adsorbates under control of thermodynamic factors and cooperative intermolecular interactions among the guest and channel surface, which most probably accompanies the molecular recognition process on the surface of the porous solid.

Acknowledgment. This work was supported in part by a Grant-in-Aid for Scientific Research from the Ministry of Education, Culture, Sports, Science and Technology, Japan.

Supporting Information Available: Crystallographic data (CIF) and ORTEP and packing views of **1**·2(EtOH) (PDF). This material is available free of charge via the Internet at http://pubs.acs.org.

IC048351S